A MICROSCALE INVESTIGATION OF NAPHTHALENE DISSOLUTION AND BIODEGRADATION

Michelle Anne Sullivan

A thesis submitted to the faculty of the University of North Carolina at Chapel Hill in partial fulfillment of the requirements for the degree of Master of Science in the Department Environmental Sciences and Engineering, School of Public Health.

Chapel Hill
2006

Dr. Frederic K. Pfaender, Advisor

Dr. Michael D. Aitken, Reader

Prof. Richard M. Kamens, Reader

ABSTRACT

Michelle Anne Sullivan: A Microscale Investigation of Naphthalene Dissolution and Biodegradation
(Under the direction of Dr. Frederic K. Pfaender)

Biodegradation of PAHs by soil microbes is often hindered because the compounds are not always available to the microorganisms responsible for metabolism. Light microscopy, with digital photography and image analysis, was used to observed naphthalene dissolution. A small scale flow cell containing a naphthalene crystal was viewed at 100x magnification. Abiotic, biotic, and azide-inhibited systems were examined in this experimental system. Changes in the crystal's mass were determined from image analysis, and changes in the aqueous naphthalene's mass were determined with a fluorescence detector. Naphthalene's mass decreased approximately 6×10^{-3} mg/hr, 1.5×10^{-3} mg/hr, and 1.0×10^{-3} mg/hr for abiotic, biotic, and azide-inhibited experiments, respectively. Cellular material around the crystal caused slower dissolution rates for the biotic and azide-inhibited experiments. There was no evidence that bacterial metabolism was occurring in the system. A model was developed which underestimated the dissolution rate by approximately one order of magnitude.

ACKNOWLEDGEMENTS

Funding for this research was provided by the Superfund Basic Research Program supported by the National Institutes of Environmental Health Sciences (Grant P42ES05948) and Small Business Technology Transfer (STTR) supported by the National Institutes of Environmental Health Sciences (Grant ES11890). I would like to thank the Pfaender/Aitken lab members for their advice, insight, and friendship. In particular, I would like to acknowledge Dr. Chad Roper, for his thoughts and suggestions that have helped shape this project. Lastly, I would like to thank my committee, Dr. Fred Pfaender, Dr. Mike Aitken, and Prof. Rich Kamens.

TABLE OF CONTENTS

LIST OF FIGURES

CHAPTER 1

INTRODUCTION, OBJECTIVES, AND REVIEW OF THE LITERATURE

1.1 - Introduction

Polycyclic aromatic hydrocarbons (PAHs) are hydrophobic organic compounds ubiquitous throughout the environment. It is important to understand the fate of PAHs because of their toxic, mutagenic, and carcinogenic properties (Menzie et al. 1992). Soil microbial communities may degrade PAHs when in a bioavailable form, but often the PAHs are not bioavailable (Bosma et al. 1997). Bioavailability can be limited by several factors such as location of the pollutant and microbe, sorption and subsequent desorption of PAHs, and the physical state of the PAHs. These factors are intertwined and understanding all these processes will help to improve strategies for the bioremediation of contaminated sites.

1.2 - Objectives

These experiments studied the interaction between bacteria and a solid PAH. Batch cultures have been used to investigate the microbial contribution to the dissolution of solid PAHs by a bacterial culture, but *in-situ* observations cannot be made using this technique (Mulder et al. 2001). This study used light microscopy to directly observe the interaction of *Pseudomonas putida* G7 and a naphthalene crystal. Three objectives were to be accomplished: 1) develop methods to use light microscopy to study naphthalene dissolution and bacterial interactions, 2) develop a model to compare information gained from image analysis and from effluent leaving the system, in order to see if a model can describe what is

occurring in the system, 3) observe differences between the abiotic and biotic experiments to see if biodegradation had a significant role during interaction.

1.3 - Polycyclic Aromatic Hydrocarbons

PAHs are organic compounds composed of fused benzene rings. Increasing numbers of fused rings increase the compound's hydrophobicity and decrease its water solubility (Aichberger et al. 2006). PAHs are formed by the incomplete combustion of organic matter with natural sources such as forest fires and volcanic eruptions (Menzie et al. 1992). However, anthropogenic contributions during the last century, namely industrial coal gasification and wood preservation, have led to numerous contaminated soils, creating public health hazards (Johnsen et al. 2005). PAHs accumulate in soil because of their physical properties, such as low aqueous solubility and high solid-water distribution ratios (Johnsen et al. 2005). The potential health risks associated with PAHs make them of great environmental concern. The EPA has identified 16 priority PAH pollutants, some of which are suspected or probable carcinogens (Menzie et al. 1992). It has been estimated that a non-smoking adult receives an average dose of 3 μg/day of carcinogenic PAH (Menzie et al 1992), with food thought to be the largest source of carcinogenic PAHs for non-smokers. However, due to their potential harmful health effects, it is important to understand the fate of PAHs in all of their environmental compartmaents (Menzie et al. 1992).

Naphthalene is the smallest PAH, consisting of two fused benzene rings. It has the highest aqueous solubility of the 16 EPA-regulated PAHs, at 31 mg/L, making it one of the most prevalent groundwater contaminants at PAH polluted sites (Marx and Aitken 1999). Naphthalene has also been demonstrated to have toxic effects on humans. The lungs and eyes are thought to be most susceptible organs, but other biomarkers such as glutathione

depletion, lipid peroxidation, DNA fragmentation and the production of active oxygen species has been shown to due to naphthalene exposure (Stohs et al. 2002). Due to its potential to contaminate groundwater and cause toxic effects, naphthalene was selected to be the PAH used in this study.

1.4 - Bioavailability

PAHs can biodegrade in soil but "their sparing solubility and tendency to form associations with organic matter greatly decrease the portion of PAH available to microorganisms" (Carmichael and Pfaender 1997). Bioavailability limitations, and not intrinsic microbial activity, appear to be the main focal point for developing more effective bioremediation strategies (Bosma et al. 1997). Bioavailability is limited by a number of circumstances with complex interactions between PAHs, soil and microorganisms and it is critical to consider all these factors to further understand the fate of PAHs in soil (Aichberger et al. 2006).

PAHs in the soil often exist absorbed to a soil particle; however, only when the PAHs are dissolved in water can they be metabolized by bacteria (Wodzinski and Coyle 1974, Stucki and Alexander 1987). When the rate of mass transfer of the pollutant to microorganisms in soil slows down, it may be an indication of reduced bioavailability (Bosma et al. 1997). Furthermore, when pollutants are completely unavailable, the rate of mass transfer is zero (Bosma et al. 1997).

Ultimately, the effectiveness of bioremediation is affected by the "physiochemical processes that control phase partitioning between solid and liquid and subsequent solute accessibility to microorganisms" (Mihelcic et al. 1993). Mass transfer mechanisms depend upon the state of the pollutant and can involve diffusion and dissolution (Bosma et al. 1997).

This study was undertaken to understand the dissolution of naphthalene to an available form for bacteria; a more in-depth look at solid-phase mass transfer is in section 3.5.

1.4.1 – Location

When pollutants enter a porous medium, they associate with macropores and particle surfaces and, over time, diffuse into smaller pores where microbial degradation can occur (Bosma et al. 1997). Microbes tend to inhabit pores that are about 0.8 – 3 μm in order to be protected from predators (Bosma et al. 1997). Contaminants may also diffuse into extremely small pores where they are no longer available to the bacteria because the microbes cannot enter the pore (Bosma et al. 1997).

A hypothesized sorption mechanism involves the PAH entering nanopores of soil organic matter (Nam and Alexander 1998). A number of soils have pores of diameters less than 100 nm and it is believed that PAHs trapped in pores of this size will be unavailable to any organism, since even the smallest bacteria are larger than 100 nm (Nam and Alexander 1998). A study by Nam and Alexander (1998) supported this hypothesis, showing that the PAH phenanthrene was sorbed most tightly to hydrophobic material with small pores and bacteria were only able to mineralize 7% of the phenanthrene absorbed, compared to 48-100% mineralization when sorbed by hydrophilic materials.

1.4.2 – Soprtion

PAHs may also sorb to soil organic matter particles, making the PAHs unavailable for biodegradation (Manilal and Alexander 1991). Different organic matter sorption traits have been observed; for example, sorption to young, uncondensed humic substance is fast, linear, and reversible whereas, absorption to condensed kerogen and black carbon is highly

nonlinear and exhibits slow sorption kinetics (Accardi-Dey and Gschwend 2002, Aichberger et al. 2006).

While the mechanisms for PAH sorption and its slow release to and from soil are not well understood, studies have been investigating sorption at the particle scale. A microprobe two-step laser desorption/laser ionization mass spectrometry study looked at 40 μm diameter circular spots on particles and noticed heterogeneity at the subparticle level and a preference of PAHs to bind to higher carbon content areas (Gillette et al. 1999). Another study using laser desorption/laser ionization mass spectrometry observed that coal/wood fractions sorbed more PAHs compared to the clay/silt fractions. A cross-section of particles indicated that sorbed PAHs were concentrated on the outer sections of the particle, indicating a near surface sorption mechanism (Ghosh et al. 2000). Other studies have supported a near surface sorption mechanism where pollutants adsorb to particles based on availability of sorbed sites and particle surface area (Luthy et al. 1997).

1.4.3 - Desorption

Sorption of PAHs to soil particles results in slow release rates back to the aqueous phase. Studies have shown that PAHs are available for biodegradation to a residual concentration that does not decrease with time or decreases slowly through years of continuous treatment (Luthy et al. 1997). The slow release rates of sorbed PAHs suggest that microbial communities are unable to act on aged PAHs until they desorb from soil particles (Carmichael et al. 1997). Over time, strong binding of PAHs to soil and slow release rates decreases not only the availability of PAHs to bacteria but also decreases the amount of PAHs available to other biota, posing less of a health threat to these organisms (Tang et al.

1998). In fact, the residual PAHs that remain might be significantly less leachable by water and less toxic (Luthy et al. 1997).

Sequestered PAHs may exist in two forms – those unavailable to any organisms and those that are differentially available, where "assimilation, toxicity, and/or biodegradation may depend on the properties of the species and its ability to mobilize the molecules from this nonremote location" (Tang et al. 1998). Therefore, sites with aged and sequestered PAHs should not be ignored due to the potential for desorption and metabolism of the PAHs over time.

While sorption and slow release rates of PAHs were not directly studied in this investigation, it is important to note that most PAHs in soil and sediment environment exist in a sorbed and/or non-aqueous phase liquid state and, eventually, microscale flow cell investigations of PAH-bacterial interactions can be used to examine real soil conditions involving similar bioavailability issues.

1.5 - Bacterial strategies

When PAHs become available to microorganisms, a concentration gradient forms and bacteria may adapt mechanisms to improve uptake of the PAHs. Some bacteria might develop an attachment mechanism to remain near or attached to the PAH source, develop high-affinity uptake systems for PAHs, or produce biosurfactants (Wick et al. 2002). A study by Wick et al. (2002) observed that *Mycobacterium* sp. LB501T cells grown on anthracene surfaces were able to adhere to Teflon and anthracene surfaces much better than glucose-grown cells. Furthermore, scanning electron microscopy showed that bacteria appeared to be attached to the crystal and formed craters, which were not present on fresh anthracene crystals (Wick at al. 2002).

Another study found green fluorescence protein-labeled *Pseudomonas putida* ATCC 17514 attaching and forming a biofilm on the crystalline surfaces of phenanthrene, but did not attach when in the presence of fluorene (Rodrigues et al. 2003). This suggests that adhesion might be controlled by the substrate availability, since fluorene is more soluble than phenanthrene (Rodrigues et al. 2003). Bacterial biosurfactant production has helped bacteria growing on other less available substrates, such as alkanes, to increase their bioavailability, but this does not seem to occur often, nor is it essential, for PAH degraders (Johnsen et al. 2005). This study examined the effect of *P. putida* G7 on naphthalene dissolution, to see if the presence of the microbe affects dissolution rates.

1.6 - Modeling bacterial-PAH interactions

Several studies have investigated the effectiveness of mass-transfer models in describing the dissolution and biodegradation processes of naphthalene (Mulder et al 1998 a-c; Mulder et al. 2001). Performing mathematical simulations of mass transfer and microbial conversion may prove useful in evaluating the potential success of and time needed for bioremediation (Mulder et al. 2001).

A stagnant film model as been used to describe the dissolution of naphthalene from stirred batch reactors (Mulder et al. 1998a). When PAHs are present in a solid form, as they dissolve a stagnant boundary layer forms where mass transfer is by diffusion (Johnsen et al. 2005). The crystal's size and shape, as well as the shaking velocity in batch cultures, dictates the thickness of the boundary layer (Mulder et al. 1998a). The boundary layer thins as the crystal size decreases and the shaking velocity increases; a thinner boundary layer increases the PAH-flux from the crystal to the bulk liquid (Johnsen et al. 2005). Outside of this

diffusive layer, mixing is assumed to be uniform due to turbulence in shaken batch cultures (Johnsen et al. 2005).

The stagnant film model assumes that mass transfer resistances are only present at the surface of a stagnant liquid film and the "concentration gradients over the film are assumed to be established rapidly in relation to changes in naphthalene in the bulk solution, so the flux throughout the film is considered constant at any given moment" (Mulder et al. 1998a). Kinetic parameters for naphthalene degradation have not been intensely studied; thus, the value of the Monod constant is often assumed (Mulder et al. 2001). Ahn et al. (1998) claim to be the first to report kinetic parameters of naphthalene degradation, and recognized their significance in improving mathematical models for degradation and transport of PAHs in soil. The kinetics of mass transfer-limited biodegradation are further explained by the Best equation, which considers the dissolution of the solid substrate and microbial degradation to calculate substrate transformation by mass transfer and microbial conversion (Bosma et al. 1997, Wick et al. 2001). Unfortunately, modeling the bacteria's effect in the flow cell was not able to be done with this study because of its complications. It is a future objective to work with modelers to predict the bacteria's role within the flow cell. This study will qualitatively look at any differences observed between abiotic and biotic data.

Stagnant film modeling has been used to examine naphthalene dissolution and degradation under a variety of conditions. In investigations of hydrodynamic conditions and nonionic surfactants, the models correlated with the experimental results, illustrating that increasing mixing and introducing surfactants increased mass transfer, making more naphthalene available for biodegradation (Mulder et al. 1998a, Mulder et al. 1998c). An examination of the effect of biofilm formation on dissolution kinetics concluded that an increase of biomass

around the crystal decreased the dissolution rate, regardless of whether the biofilm was active or not (Mulder et al. 1998b). Furthermore, mathematical manipulations of these models, factoring in biofilm formation, supported the assertion that bioavailability of solid naphthalene is always reduced in the presence of a biofilm (Mulder et al. 1998b).

Models may also examine PAHs in various physical states (such as pure crystal, pure solid in a pore, and sorbed in a soil aggregate) to determine the period needed to achieve PAH removal (Mulder et al. 2001). Modeling provides valuable insight into the optimal mass-transfer parameters for efficient bioremediation; however, further evaluation of PAH physical states in real soil matrices is necessary to validate the proposed models (Mulder et al. 2001). The models discussed here were used develop the models used for our system, which uses a flow cell instead of a batch reactor, to examine naphthalene dissolution and biodegradation.

1.7 - Microscope Applications

Microscopy has proven to be useful for evaluating microbial relationships with PAHs. A study by Amellal et al. (2001) used transmission electron microscopy to gain insight into the location and distribution of PAHs and bacteria in soil. Image analysis showed that, while bacteria were located near high PAH concentrations in fine silt and clay aggregates, over time the PAH degradation was limited, indicating that soil particle organization and structure of soil aggregates play an important role in degradation (Amellal et al. 2001). A batch culture was observed for 4 months using light microscopy to track its growth and differences in the microbial community were tracked by molecular techniques (Eriksson et al. 2002).

Using flow cells in conjunction with microscopy should improve our understanding of bacteria's preferences for metabolizing hydrophobic compounds, such as PAHs (Rodrigues

et al. 2003). Additionally, flow cells have been used to understand biofilm formation and possible environmental factors that trigger biofilm formation, such as starvation and influences of hydrodynamics (Hunt et al. 2004, Purevdorj et al. 2002). The flow cell used in most other experiments have large dimensions, such as 5 x 10 x 40 mm, when compared to the flow cell used in this investigation, where the dimensions are 0.3 x 0.3 x 1 mm. Using microscopy and flow cells will allow us to visualize interactions between bacteria and solid PAHs to perhaps gain further insight about PAH degradation that cannot be observed with batch reactor experiment.

CHAPTER 2

METHODS AND MATERIALS

2.1 - Media Preparation

M9 media was modified from Miller (1972) with a 10 fold reduction in concentration of $MgSO_4 \cdot 7\ H_20$ and $CaCl \cdot 2\ H_20$ to improve solubility. M9 media consisted of 3 g KH_2PO_4, 1 g NH_4Cl, 0.5 g NaCl, 0.014 g $CaCl \cdot 2\ H_20$ (Mallinckroft, Paris, KN), 6 g Na_2HPO_4, and 0.025 g $MgSO_4 \cdot 7H_20$ (Fischer Scientific, Fair Lawn, NJ) per liter of water with a pH of 7, and 5mM sodium salicylate (Mallinckroft, Paris, KN) was added as an energy source. To conduct azide inhibited experiments, 0.1% (weight: volume) of sodium azide added was added to the M9 media. Tryptone broth was made with 10 g of tryptone (Difco, Sparks, MD) and 5 g of sodium chloride (Mallinckroft, Paris, KN) per liter of water as described in Marx and Aitken (1999). A 1mM indole (Aldrich, St. Louis, MO) solution was prepared to stain *Pseudomonas putida* G7 blue for visualization under the microscope.

2.2 - Culture Conditions

Frozen stocks of wild type *Pseudomonas putida* G7 (obtained from laboratory of Dr. Michael D. Aitken, University of North Carolina – Chapel Hill) were stored at -20° Celsius. Using a sterile wooden applicator stick, a scrape of the frozen stock with was suspended in 5 mL of tryptone broth. The inoculated broth was incubated at 25° Celsius with shaking (250 rpm) for 24 hours. To induce the *nah* gene for naphthalene biodegradation, 1 mL was transferred to 20 mL of M9 media with 5 mM sodium salicylate and 10 mL of 1 mM indole

solution. When the *nah* pathway is active, *P. putida* G7 will convert the indole to indigo and stain the cells blue, which is useful both as an indication of activity and for observation with the microscope. The bacteria grew until early stationary phase (16-18 hours), where the optical density was between 0.663 and 0.789 at 590 cm^{-1} wavelength with a cell density around 10^8 cells/mL. The stage and density of the organisms was determined by a growth curve (see Appendix 1). The bacterial culture was centrifuged for 5 minutes at 3500 rpm, the supernatant decanted, and the cell pellet was re-suspended in either M9 media with 5 mM sodium salicylate (for biotic experiment) or M9 media with 5 mM salicylate and 0.1% sodium azide (for azide inhibited experiment). The solution was then placed in a 30 mL plastic syringe (Fischer Scientific, Fair Lawn, NJ). Experiments consisting of unstained biotic and azide inhibited conditions were conducted and the growth conditions for these experiments were the same as mentioned above except the cells were grown in the presence of 30 mL of M9 containing sodium salicylate with no indole solution.

2.3 - Experimental equipment

2.3.1- Flow cell

The flow cell, shown in Figure 2.1, consisted of a 5-cm long square borosilicate glass capillary (300 um internal dimension, Vitrocom, Morris Lakes, NJ) glued (The Amazing Goop, Eclectic Products, Eugene, OR) onto a 25x75 mm glass cover slip (Bellco, Vineland, NJ). A naphthalene crystal (Aldrich, St. Louis, MO) was placed in the capillary tube and two 31 gauge, 6 inch needle "wires" (Small Parts, Miami Lakes, FL) of 0.005" (approximately 0.1 mm) internal diameter spaced approximately 1 mm apart were glued into the capillary ends (Loctite Instant Glass Glue, Avon, OH). The needle wires had a two-inch

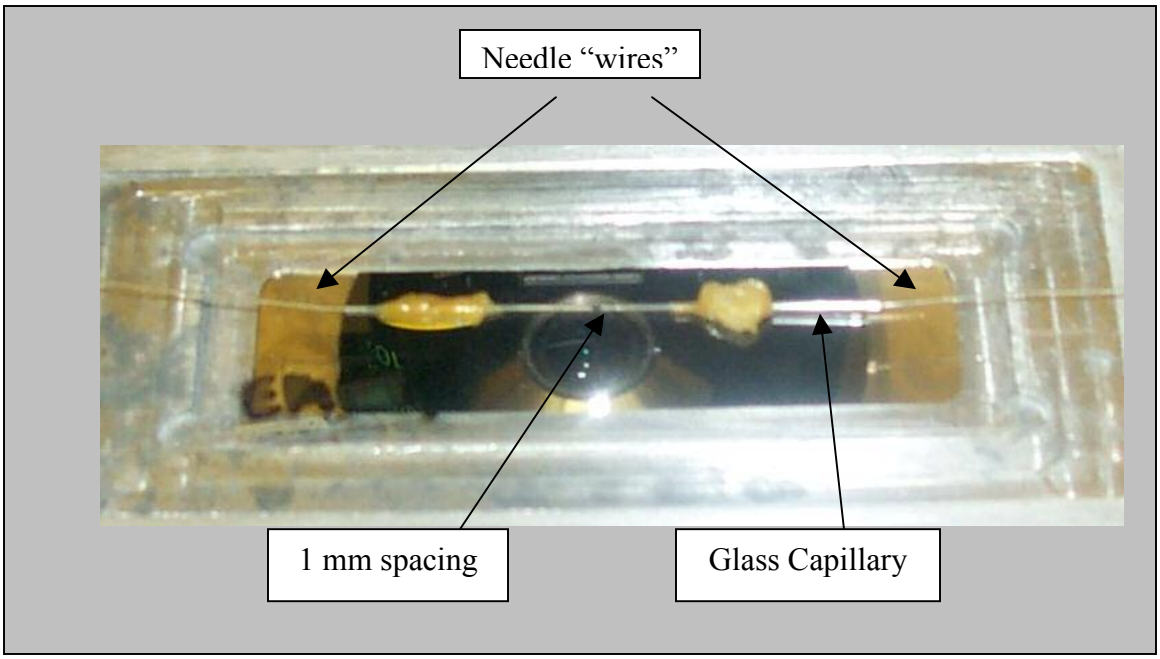

Figure 2.1: Flow cell on microscope stage.

piece of 0.010” internal diameter Peek HPLC tubing glued to the ends, allowing the system to be connected to the syringe pump (Harvard Apparatus, Natick, MA) and fluorescence detector (Shimadzu RF-530, Columbia, MD) with HPLC fittings.

2.3.2 - Microscope

Images were collected using an Olympus IX 71 Inverted Epifluorescence microscope (OPELCO, Dulles, VA) with a CCD camera. The images collected used bright field light and all images in these experiments were taken at 100x magnification.

2.3.3 - Fluorescence Detector

The effluent leaving the flow cell flowed directly into the Shimadzu Fluorescence Spectromonitor RF-530, set to observe any naphthalene present in solution (excitation - 282 nm and emission - 336 nm). The fluorescence detector was calibrated in order to determine the concentration of naphthalene associated with a given volt reading from the detector (see Appendix 2). The fluorescence detector data were collected with the DI-148 U data acquisition set (DATAQ Instruments, Akron, OH), which included an analog box with a

USB cord to send information from the fluorescence detector to the computer. The DI-148 set included the WINDAQ software (DATAQ Instruments, Akron, OH) to collect and analyze the fluorescence data on the computer.

2.4 - Experimental procedure

The flow cell containing a naphthalene crystal was placed on the stage of the microscope. The syringe pump delivered media from a 30-mL plastic syringe at a rate of 0.01 mL/min via the HPLC fitting connected to the needle wire end. Abiotic experiments used M9 media with sodium salicylate and azide, biotic experiments used *P. putida* G7 suspended in M9 media with sodium salicylate, and azide-inhibited experiments added azide to the biotic solution. The effluent from the flow cell was connected to the fluorescence detector and pictures were taken every ten minutes by a CCD camera until the naphthalene crystal was dissolved. The experimental setup is shown in Figure 2.2.

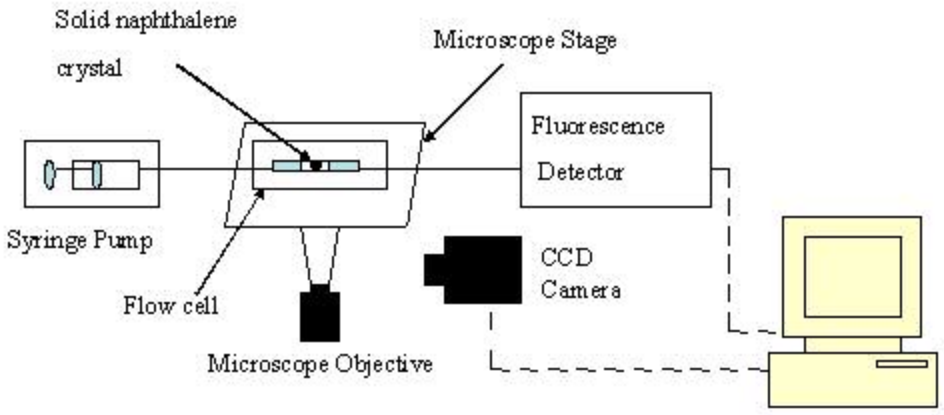

Figure 2.2: Setup for the experiments

2.5 - Data Analysis

TIFF images were captured using an Olympus Microfire™ 2.1 megapixel 12-bit camera and analyzed using Adobe Photoshop™ (CS or 7.0) with Reindeer Graphics' Fovea Pro™ image analysis plug-in. These software packages provide automated batch measurement of image features, including equivalent diameter. Figure 2.3 shows how the equivalent diameter was determined. The original image had the area around the crystal selected for, in order to

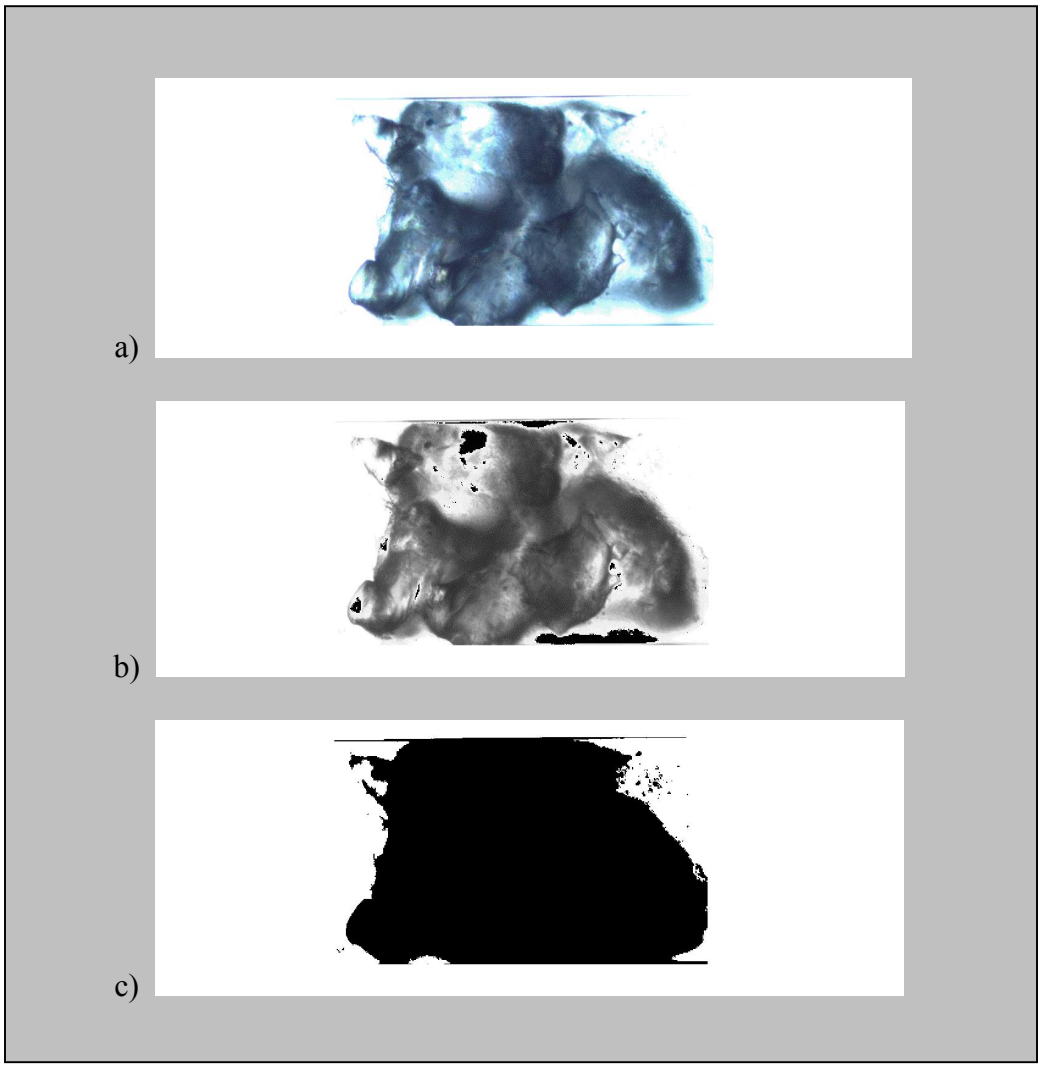

Figure 2.3: Image analysis processing a) image after area selection, b) grayscaled image, and c)binary image.

attempt to ignore bubbles in the system, and then the image was converted to grayscale. Next, the image was converted to a binary image in order to measure the diameter and other features which were sent to a spreadsheet file. The image software was calibrated to measure the diameter in micrometers (μm). The diameter measurements were converted to surface area to observe dissolution over time.

The formation of bubbles caused a shadow that resulted in an overestimation of crystal size when the microscopic image was converted to a binary image for analysis as shown in Figure 2.4. Pictures where bubbles were casting a shadow were not analyzed. The picture analysis was compared to results measured by the fluorescence detector.

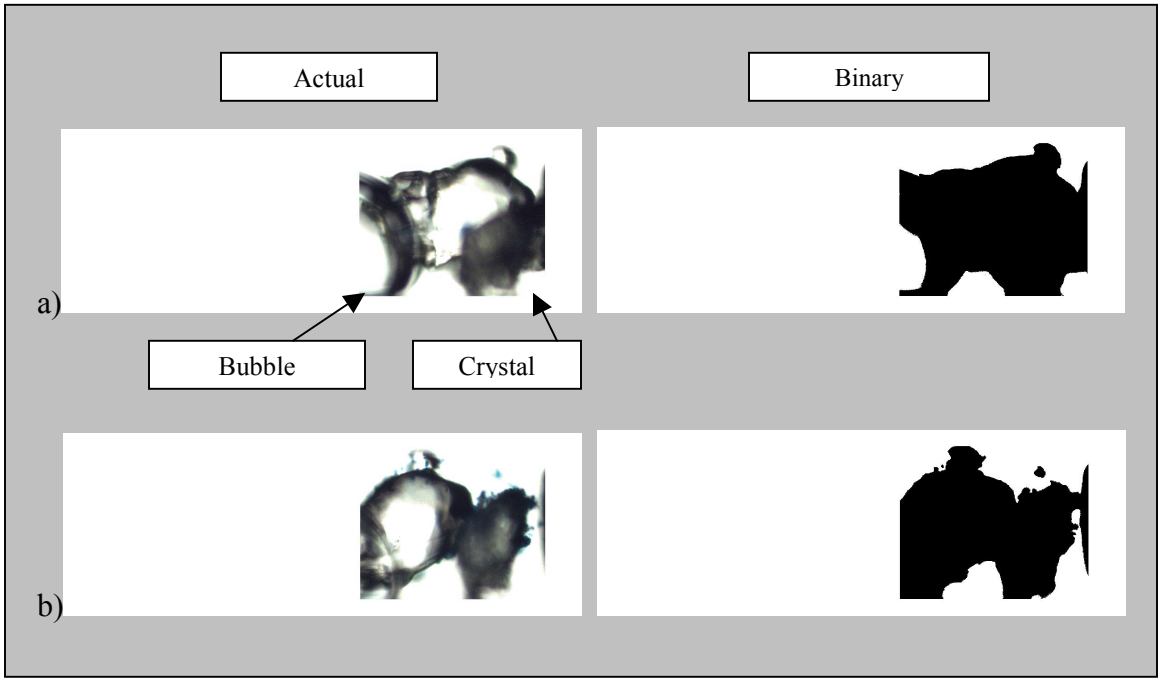

Figure 2.4: Actual and binary image a) with bubbles and b) without bubbles

2.6 – Model Development

A model was developed for the flow cell to determine the changes in surface area over time. The model used the correlation of the Sherwood, Reynolds, and Schmidt numbers, shown in equation 1, to determine the mass transfer coefficient (k) for naphthalene dissolution in water (equation 2) (Bird et al. 1960, Fogler 2006).

$$Sh = 2 + 0.6\,Re^{0.5}\,Sc^{0.333} \quad (1)$$

where Sh is the Sherwood number = $\frac{kd_p}{D_N}$

Re is the Reynolds number = $\frac{v\rho_w d_p}{\mu_w}$

Sc is the Schmidt number = $\frac{\nu_w}{D_N}$

k = mass transfer coefficient for naphthalene dissolution into water
d_p = particle diameter (cm)
ρ_w = density of water = 0.9982 g/cm^3 at 20 ºC
$\mathcal{D}_N$ = diffusivity of naphthalene in water = 8.5 x 10^{-6} cm^2/s (Marx and Aitken, 1999)
v = flow velocity = 0.185 cm/s (0.01 mL/min in a square channel with 0.3 mm sides)
μ_w = viscosity of water = 1.002 x 10^{-3} N s m^{-2} at 20 ºC = 0.01 g s^{-1} cm^{-1}
υ_w = kinematic viscosity of water = 1.003 x 10^{-6} m^2/s at 20 ºC = 0.01 cm^2/s (Aitken, personal communication).

The k value was determined using the following equation:

$$k = \frac{\left(1 + 19.246 r_p^{0.5}\right) D_N}{r_p} \text{ in cm/s} \quad (2)$$

where k= mass transfer coefficient (cm/s)
r_p = particle radius (cm)
$\mathcal{D}_N$ = diffusivity of naphthalene in water = 8.5 x 10^{-6} cm^2/s (Marx and Aitken, 1999)
(Aitken, personal communication).

A mass balance equation was needed to observe changes of naphthalene in the solid and aqueous phases. The model assumes the naphthalene particle is spherical and the aqueous phase around the particle is well-mixed, indicating the bulk naphthalene concentration is unifrom around the particle and is equal to the concentration exiting the flow cell (Aitken, personal communication). The aqueous phase mass balance equation is:

$$-QC + kA(C^* - C)V = V\frac{dC}{dt} \text{ or } \frac{dC}{dt} = kA(C^* - C) - \frac{C}{\tau} \quad (3)$$

where Q = flow rate (cm^3/s)
C = bulk aqueous-phase concentration of naphthalene (g/cm^3)
A = particle surface area (cm^2)
C^* = saturation concentration of naphthalene in water
V = volume (cm^3)
τ = residence time (s)

(Aitken, personal communication).

The mass balance on naphthalene in the solid phase is:

$$\frac{dM}{dt} = -kA(C^* - C) = -k\left(4\pi r_p^{\,2}\right)(C^* - C) \quad (4)$$

where M is the total mass of naphthalene

(Aitken, personal communication).

The radius of the particle is the major variable with time, therefore it is important to solve the model for radius, as opposed to mass. The change of radius over time is:

$$\frac{dr_p}{dt} = -\frac{k(C^* - C)}{\rho_N} \quad (5)$$

where ρ_N is the density of solid naphthalene (1.025 g/cm^3 at 20 ºC)
(Aitken. personal communication).

To solve for changes in surface area instead of radius, the following equation was needed:

$$\frac{dA}{dt} = \frac{dA}{dr_p}\frac{dr_p}{dt} \quad (6)$$

$$\frac{dA}{dr_p} = 8\pi r_p \tag{7}$$

where A = surface area (cm^2)

Changes in the naphthalene's surface area over time were estimated by modeling the following equation:

$$\frac{dA}{dt} = -(8\pi)\left(1 + 19.246 r_p^{0.5}\right)\frac{D_N f}{\rho_N} \tag{8}$$

Where A = surface area (cm^2)
f = C^* - C (g/ cm^3)
(Aitken personal communication).

CHAPTER 3

RESULTS

3.1 – Introduction

Experiments were conducted to investigate the use of microscopy to evaluate naphthalene dissolution and biodegradation, either in the absence or presence of naphthalene-degrading bacteria. The images collected from the microscope were analyzed and compared to data acquired from the fluorescence detector. The experimental results were used to evaluate a model designed to simulate the flow cell system.

3.2 – Abiotic Results

The abiotic experiments served to observe naphthalene dissolution in the system without bacterial influences. We used two methods, image analysis and fluorescence detection, to collect data on the dissolution of naphthalene. During image analysis, changes in crystal size were quantified from images taken from the microscope in 10-minute intervals. Fluorescence detection relied on measuring aqueous concentrations of naphthalene present in the effluent by flowing the effluent from the flow cell directly into a fluorescence detector.

The resulting data from these two methods were converted into mass units to compare the crystal's mass lost from dissolution (image analysis) to the cumulative mass of naphthalene in the aqueous phase present in the effluent (fluorescence detection). Conservation of mass would predict that the initial mass of the crystal would be the same as the cumulative mass of aqueous phase naphthalene after dissolution was complete. None of the crystals used in the

three experimental runs had the same surface area prior to experimentation; thus, once the crystals dissolved to a similar surface area (the "initial area"), data from this point were used to compare each run. The initial crystal areas for data collection were 7.26 x 10^{-3}, 7.34 x 10^{-3}, and 7.46 x 10^{-3} cm^2. Figure 3.1 shows the results for the abiotic experiments. According to image data, the crystals dissolved at a rate of 6.14 x 10^{-3} +/- of 0.39 x 10^{-3} mg/hr, while aqueous naphthalene mass appeared in effluent, according to the fluorescence detector, at a rate of 2.65 x 10^{-3} +/- 0.01 x 10^{-3} mg/hr. The fluorescence detector underestimates the naphthalene mass by about a factor of 2 compared to the image analysis. The fluorescence detector data might underestimate the crystal size because pieces of the

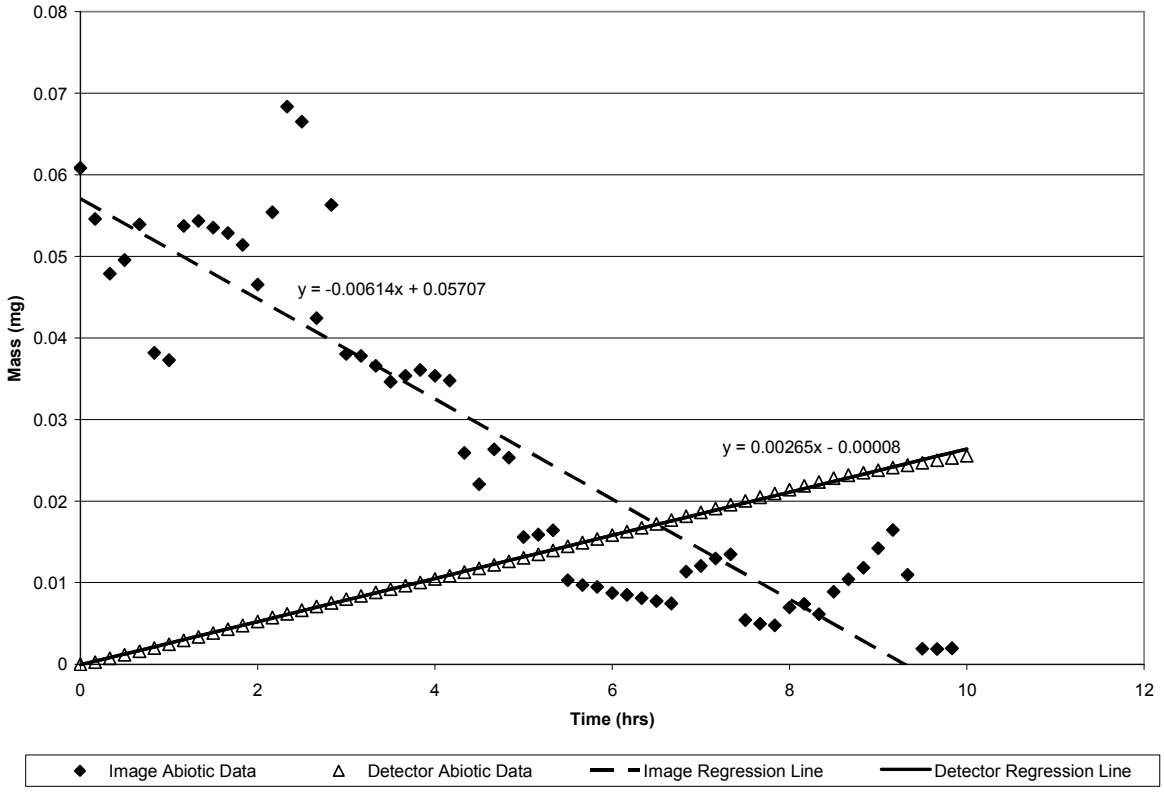

Figure 3.1: Abiotic mass lost from the crystal (images) and present in aqueous solution (fluorescence detector).

crystal had broken off, which do not dissolve into an aqueous state in the effluent, so they would not be measured by the detector.

3.3 – Biotic Results

Biotic experiments intended to investigate bacterial influence on dissolution by introducing stained *P. putida* G7 into the solution, and then comparing the dissolution rate to abiotic and azide-inhibited runs. Like the abiotic runs, crystals with similar surface areas in the four runs were used for comparison, with initial surface areas of 3.62×10^{-3}, 3.63×10^{-3}, 3.65×10^{-3}, 3.66×10^{-3} cm^2. Figure 3.2 shows that dissolution occurred at 1.46×10^{-3} +/- 0.04×10^{-3} mg/hr according to image analysis and the detector observed an increase in aqueous naphthalene mass at a rate of 1.23×10^{-3} +/- 0.03×10^{-3} mg/hr. The two

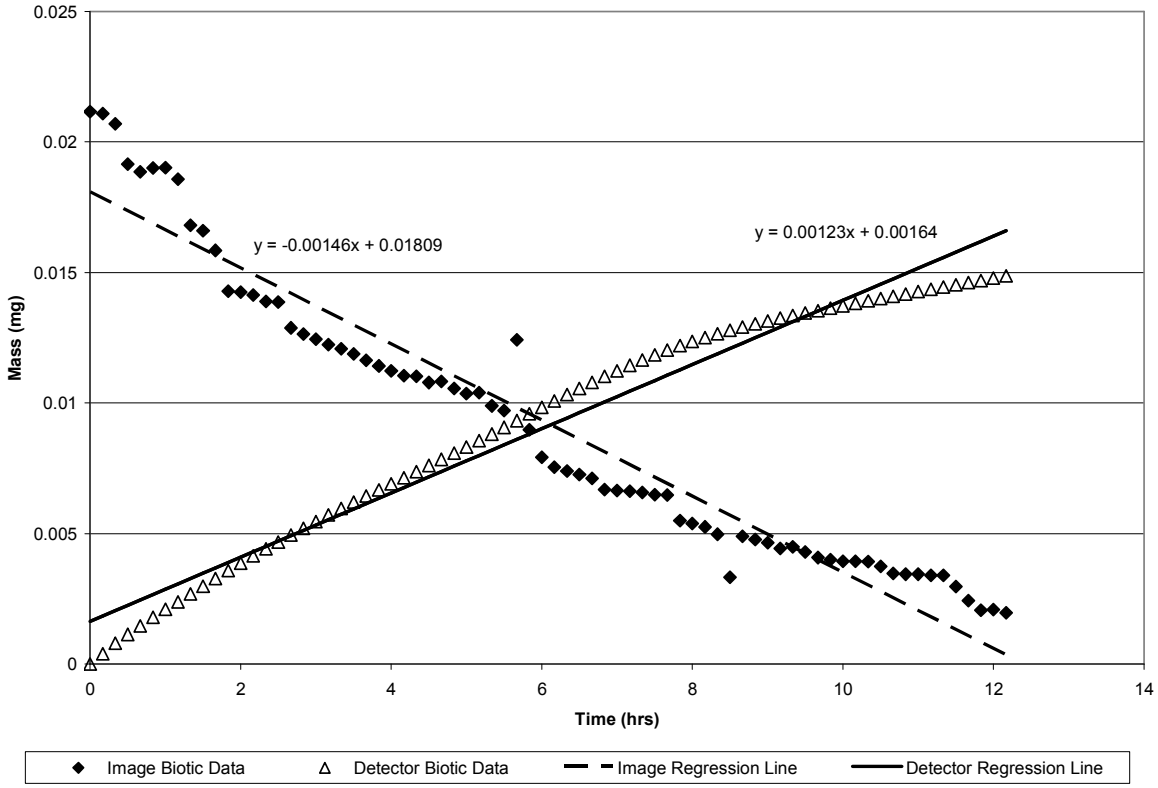

Figure 3.2: Biotic mass lost from the crystal (images) and present in aqueous solution (fluorescence detector).

measurement methods are comparable, which indicates that an accumulation of biomass due to the bacteria may have shielded the crystal from flow and prevented the crystal breakage which seemed to occur with abiotic runs. Differences in the rates were not observed, indicating that the bacteria did not metabolize a quantifiable amount of naphthalene. This could be because total dissolution occurred quickly (within 10 hours), so the bacteria may not have had enough time to metabolize a significant amount of the crystal.

3.4 – Azide-inhibited Results

As a control of the biotic experiments, additional experiments were conducted in which biomass was introduced to the flow cell but was inhibited by azide. If the biotic results differed from the azide-inhibited controls, it would indicate that metabolic processes occurred in the flow cell during the biotic runs and that the differences from the abiotic runs were not simply due to the accumulation of biomass. The initial surface areas were similar once again - 4.15×10^{-3}, 4.53×10^{-3}, and 4.64×10^{-3} cm^2 and the results are shown in Figure 3.3. The crystal dissolved at a rate of 0.95×10^{-3} +/- 0.04×10^{-3} mg/hr and the amount of aqueous naphthalene appearing in the effluent occurred at a similar rate, 1.30×10^{-3} +/- 0.02×10^{-3} mg/hr. These rates are similar to the biotic experiments. The bacteria were inhibited from metabolizing naphthalene during these runs because of the azide; therefore, the similarity of their results to the biotic runs shows that biological activity was probably not occurring within the flow cell during the biotic experiments.

The biotic and azide-inhibited runs had slower dissolution rates than abiotic runs (about 1.0×10^{-3} mg/hr compared to 6×10^{-3} mg/hr) because the presence of cellular material around the crystal impeded dissolution. Furthermore, the material around the crystal most likely made it more difficult for crystal pieces to break off, as in the abiotic runs, since it provides a

shield from the flowing aqueous solution. Thus, unlike the abiotic runs, the fluorescence data for the biotic and azide-inhibited runs observed conservation of mass.

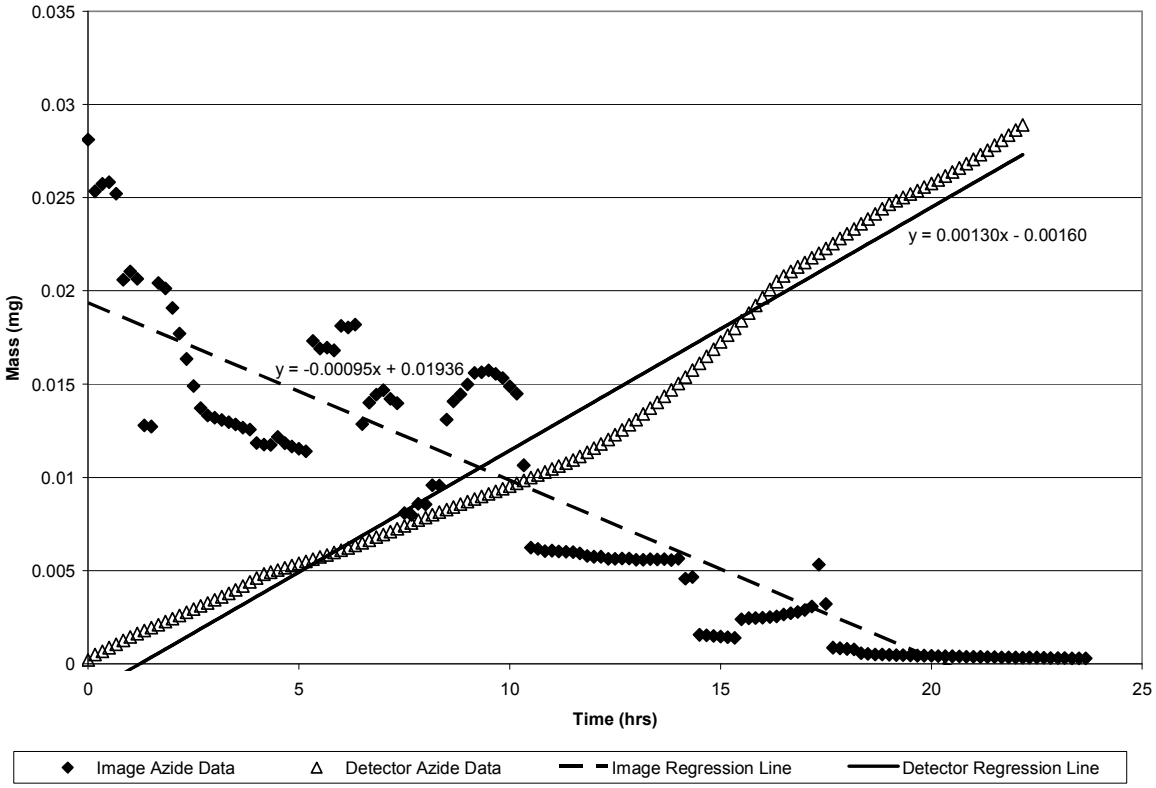

Figure 3.3: Azide-inhibited mass lost from the crystal (images) and present in aqueous solution (fluorescence detector).

CHAPTER 4

DISCUSSION

4.1 - Introduction

The objectives of this work were: 1) to develop a new method for observing bacterial-PAH interactions, 2) to build a model that could predict naphthalene dissolution in the flow cell, and 3) to observe differences between the abiotic and biotic conditions within a flow cell. Each of these objectives were met and provided valuable information for improving this investigation for the future.

4.2 – Method Development

The flow cell was designed so that microscale observations could be obtained in a controlled environment. The flow cell, in conjunction with microscopy, allowed for naphthalene dissolution and biodegradation processes to be observed directly. Previous experiments (Mulder et al. 1998 a-c, 2001) used batch cultures, but this approach does not simulate real soil conditions where water flow could continuously pass around a crystal. Direct observations of the crystal size cannot be made, instead dissolution rate is determined by measuring aqueous concentration (Mulder et al. 1998 a-c, 2001). The flow rate chosen for this experiment was limited by the syringe pump and provided faster flow conditions than those seen under real conditions, which usually vary from 0.001 m/day to 10m/day (Alexander and Fairbridge 1999), but it did, however, allow for the methods to be tested and microscale observations to be made.

Overall, the flow cell provided a unique way to study naphthalene dissolution and biodegradation processes. The small size of the flow cell allows for a controlled environment and the use of the flow cell and microscopy provides a valuable tool in studying bacterial processes with PAHs. Future work should use more realistic flow velocities and eliminate bubbles from the system make the design more relevant and accurate.

4.3 – Model development

The surface area model results were converted to mass lost over time for the minimum (3.62×10^{-3} cm^2) and maximum (7.46×10^{-3} cm^2) initial surface areas used and the results are presented in Figure 4.1.

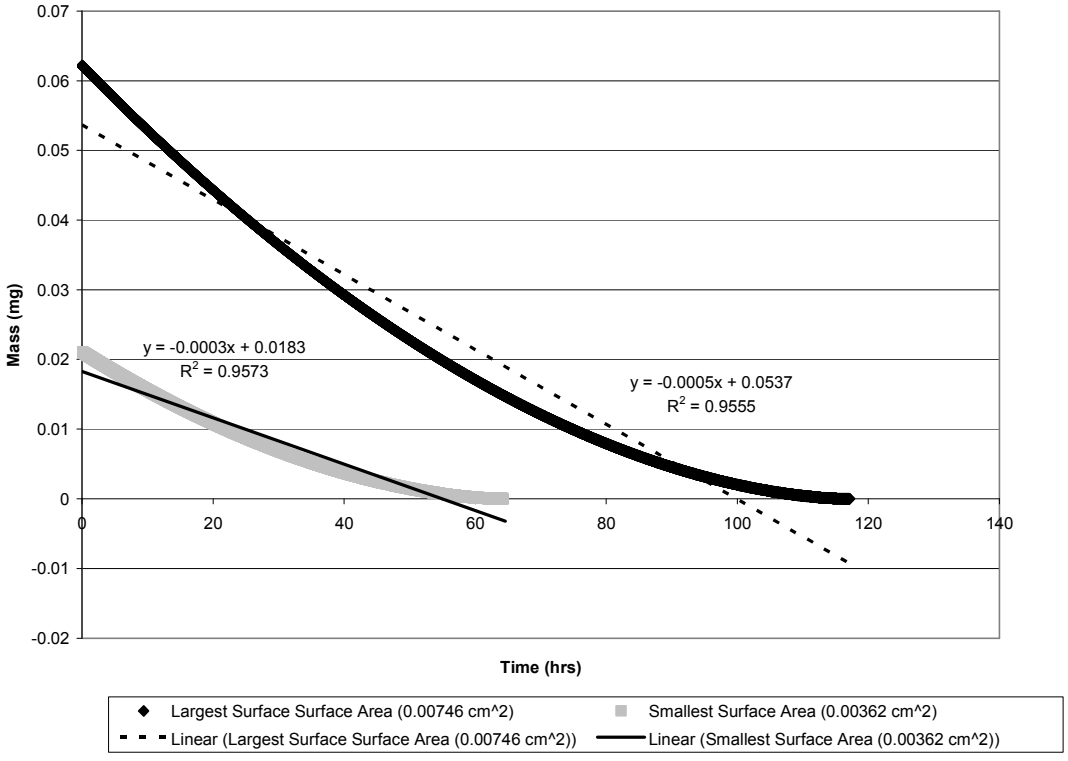

Figure 4.1: Model predicting mass changes for naphthalene

The model predicts dissolution to take place at a rate of 3.0×10^{-4} to 5.0×10^{-4} mg/hr, depending upon the size of the crystal. The experimental rates were one order of magnitude

faster, so the model does not simulate the experimental results well. The model was based on the mass transfer and flow conditions, which is calculated based on the Sherman, Schmidt, and Reynolds numbers, and assumes the naphthalene crystal to be a singular, perfect sphere, which was not the case experimentally. The crystal was often non-symmetrical and, on some occasions, present in several pieces at various points in time. In the case of the latter, the surface areas of the pieces were summed to represent the equivalent of one crystal for each time point. The smaller pieces with smaller surface areas may have dissolved more rapidly as separate pieces than one larger equivalent crystal, which could have been a cause for the model's overestimation of the time needed for complete dissolution. The smaller pieces have a larger surface area relative to their mass, so there is more area exposed to flow and less mass to deteriorate. The model did not take into consideration the effect of the internal diameter difference between the needle and the flow cell. The change between internal diameters that the solution encountered as it flowed through the system could cause turbulent conditions, promoting mixing and possibly affecting the stagnant film layer created by biomass accumulation that influences the mass transfer rate. Consideration of these experimental differences could aid in more accurately predicting experimental results.

A previous study attempted to model naphthalene dissolution in batch cultures, varying the hydrodynamic conditions to observe if the model was supported by experimentation (Mulder et al. 1998a). This model was formed using concepts similar to those discussed here, though the batch culture hydrodynamics resulted in a different mass transfer coefficient. The flow velocities in the batch culture system were small enough to ignore the Reynolds and Schmidt numbers when calculating the mass transfer coefficient (Mulder et al. 1998a). Unlike our model, the Mulder model's predictions were very close to what was observed experimentally

(Mulder et al. 1998a). Developing models using simple systems such as batch cultures can provide useful information, but it indirectly determines naphthalene dissolution by measuring naphthalene concentration in the effluent. While it is a more complex system, the flow cell directly observes changes in the naphthalene crystal to determine the dissolution rate which provides a more accurate idea of processed occurring during dissolution.

4.4 – Observations between abiotic and biotic experiments

Abiotic experiments were conducted to determine the dissolution rate of naphthalene without any bacterial influence. The biotic experiment introduced *P. putida* G7 to observe any biodegradation effects on the naphthalene, and the azide inhibited experiment used sodium azide to inhibit *P. putida* G7 and ensure that any effects observed in the biotic run were due to biological metabolism.

As seen in Figure 4.2, there are differences between the three experiments in the study. Figure 4.2a shows that naphthalene dissolved much faster in the abiotic experiment than in the biotic or azide-inhibited runs, as the abiotic run began with a much larger crystal than the other runs and after 5 hours had the smallest crystal remaining. In the biotic and azide-inhibited experiments, cellular mass accumulated around the crystal, which slowed down the dissolution rate, as seen in Figure 4.2b and c. There is a difference between biotic and azide-inhibited runs, though, because the azide-inhibited bacteria appear to clump together, causing a greater accumulation of cellular material around the crystal.

As indicated by the graphs presented in the results section, the dissolution process of naphthalene between the abiotic and biotic experiments was different. Abiotic dissolution proceeded at a much faster rate than the biotic or azide-inhbited dissolution, which is expected due to cellular material surrounding the crystal hindering dissolution. The biotic

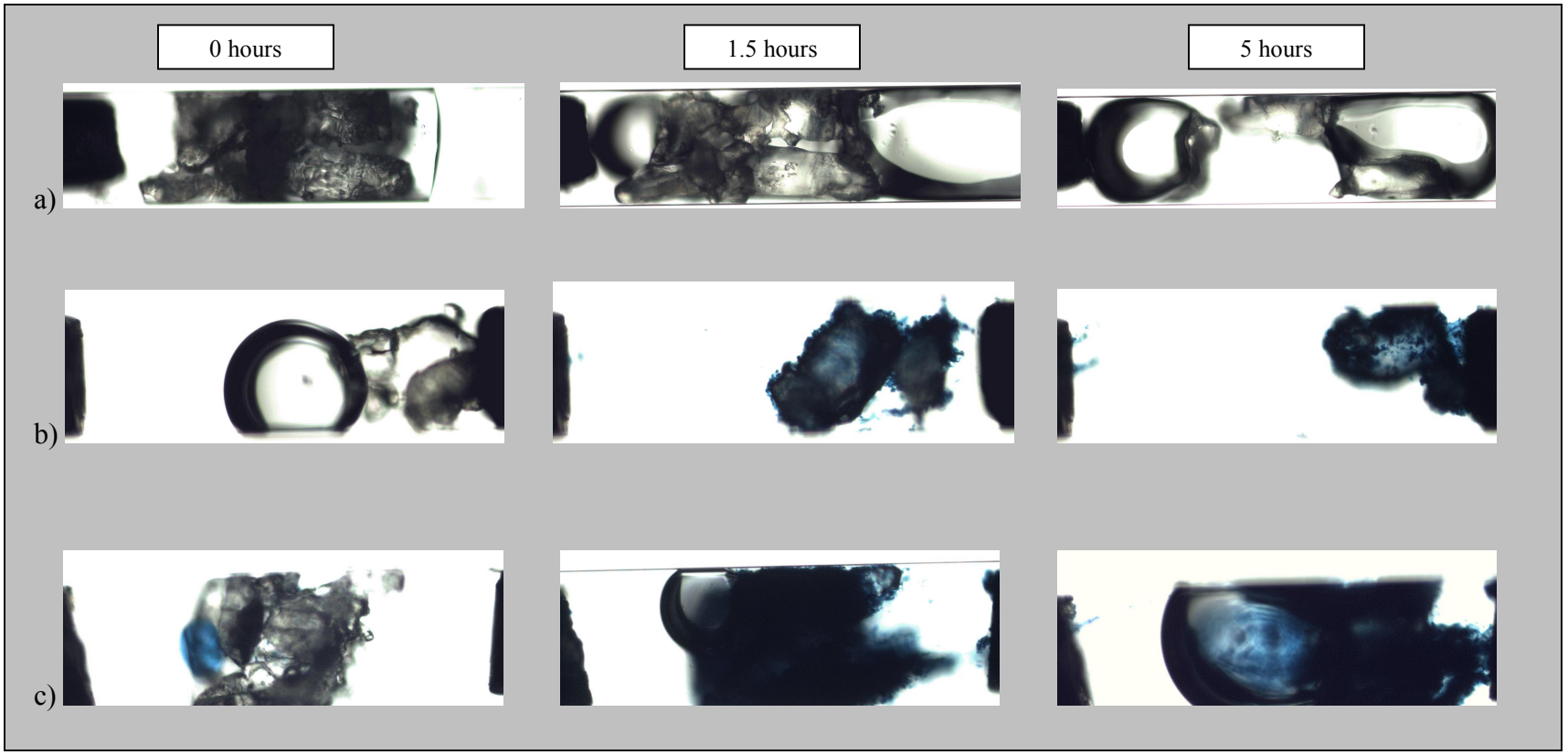

Figure 4.2: Pictures taken at 0, 1.5, and 5 hours during (a)abiotic, (b)biotic, and (c)azide inhibited experiments

runs did not display a difference in lost mass as measured by image analysis and fluorescence detection. If *P. putida* G7 were metabolizing the crystal, one would expect there to be less naphthalene present in the aqueous phase than in the original crystal because the bacteria were consuming some of the dissolved naphthalene. Since there was no mass difference between the solid and aqueous phase of naphthalene for the biotic runs, it appears the cells were not metabolizing naphthalene. Additionally, azide-inhibited experiments had similar dissolution rates to biotic experiments, providing further evidence that little biological activity occurred in the biotic flow cell.

4.5 – Overall Conclusions

- To our knowledge, this is the first use of the microscale flow cell to study naphthalene dissolution and biodegradation. There are some operational parameters that need improvement, mainly the introduction of bubbles into the system and the high flow velocities.
- Unlike modeling for naphthalene dissolution in batch cultures (Mulder et al. 1998a), the flow cell system did not produce results that agree with a model based on mass transfer and fluid flow. The model used overestimated the experimental dissolution time for naphthalene by one order of magnitude. Possibly, the difference could be that the flow cell frequently had many small naphthalene crystals and the model assumed one large crystal was present in the flow cell. The smaller pieces would dissolve faster, resulting in a faster erosion of the crystal's mass than what is predicted by the model.
- Changes in naphthalene mass over time were monitored two ways, microscopically using image analysis of the remaining crystal and analytically measuring the effluent

using a fluorescence detector. When the two methods were compared, the image analysis predicted a larger naphthalene particle than the fluorescence detector for the abiotic experiment. It is possible that pieces of the naphthalene crystal broke off and entered the fluorescence detector and the instrument was not able to record this result. The two methods predicted similar size naphthalene particles for biotic and azide inhibited experiments, which indicates bacterial metabolism is not occurring at an influential rate.

Appendix I

Growth Curve

A growth curve was done to determine the stage and concentration of P. putida G7 as it grew in M9 media with salicylate and indole. The bacteria were grown using the same methodology described in section 3.2, except once 1 mL of inoculated tryptone broth was placed in the M9 media sampling at various time points occurred for the next 24 hours. At a sample time point, the inoculated M9 media had its optical density measured at a wavelength of 590 nm and a diluted sample was plated on LB plates. Our main interest was to quantify the bacteria present around 16-18 hours, because within this time period was when the bacteria were introduced into the flow cell. Figure A1.1 shows optical density curve and Figure A1.2 shows the microbial growth curve. Between 16-18 hours, the bacteria appear to be have reached early stationary phase, with an optical density of 0.80 and 0.85 cm^{-1} and a cell concentration of about 1.2 x 10^8 cells/mL.

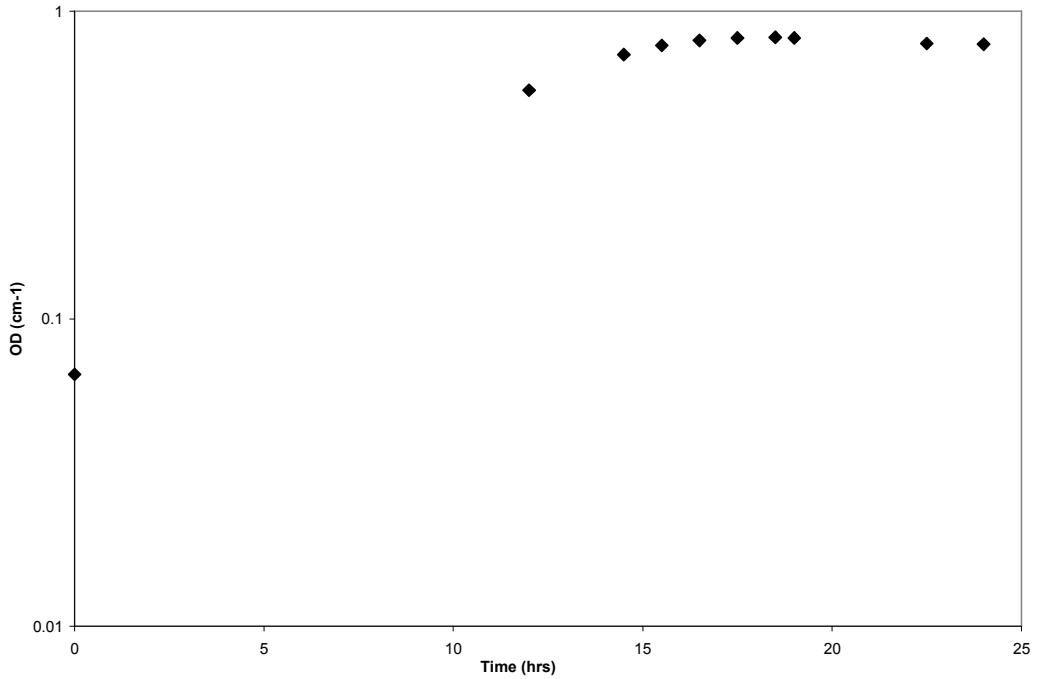

Figure A1.1: Optical density over 24 hours for *P. putida* G7

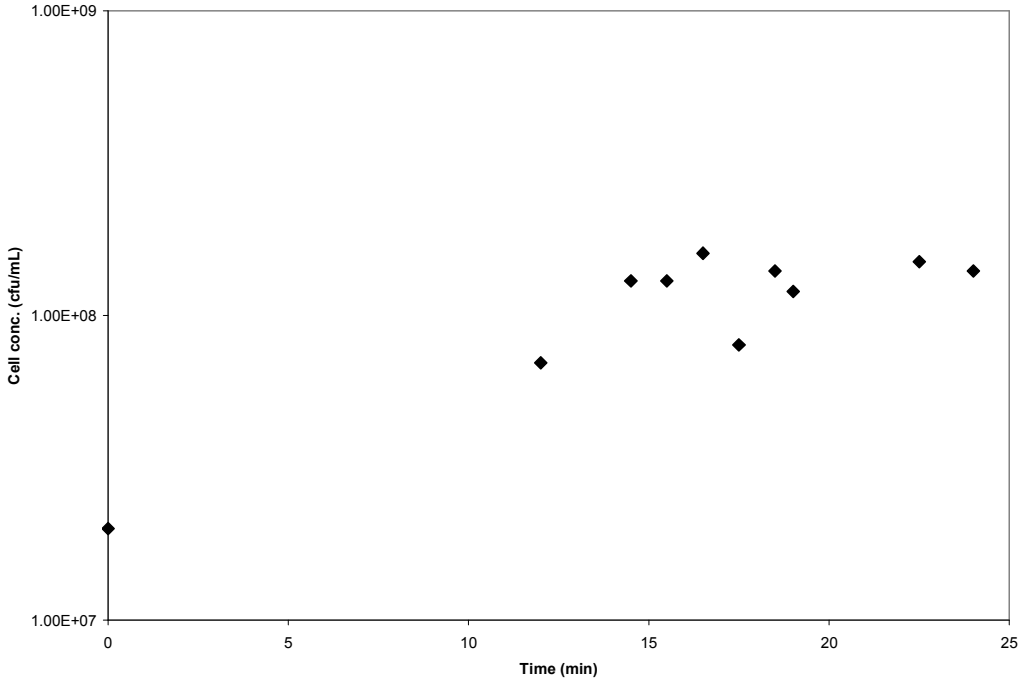

Figure A1.2: Cell concentration over 24 hours for *P. putida* G7

Appendix II

Fluorescence Detector Calibration

To calibrate the fluorescence detector, naphthalene solutions with the concentrations of were flown thought the detector at a rate of 0.1 mL/min, for 15 minutes each concentration. This amount of time allowed a nice flat output line to form, and the arbitrary units was recorded. The arbitrary units for the detector were standardized so that the initial concentration was at 0 mg/L, since sometimes when no naphthalene was being flown the read out was above or below zero. All of the concentrations were flown through 5 times, and then a plot of naphthalene concentration verses voltage output was graphed (Figure A2.1), and a linear relationship was observed (r2 = 0.9784). The linear equation, y = 1.4282x (where y represents the arbitrary units and x represents the naphthalene concentration) was used to change voltage readings to concentration values for effluent leaving the flow cell.

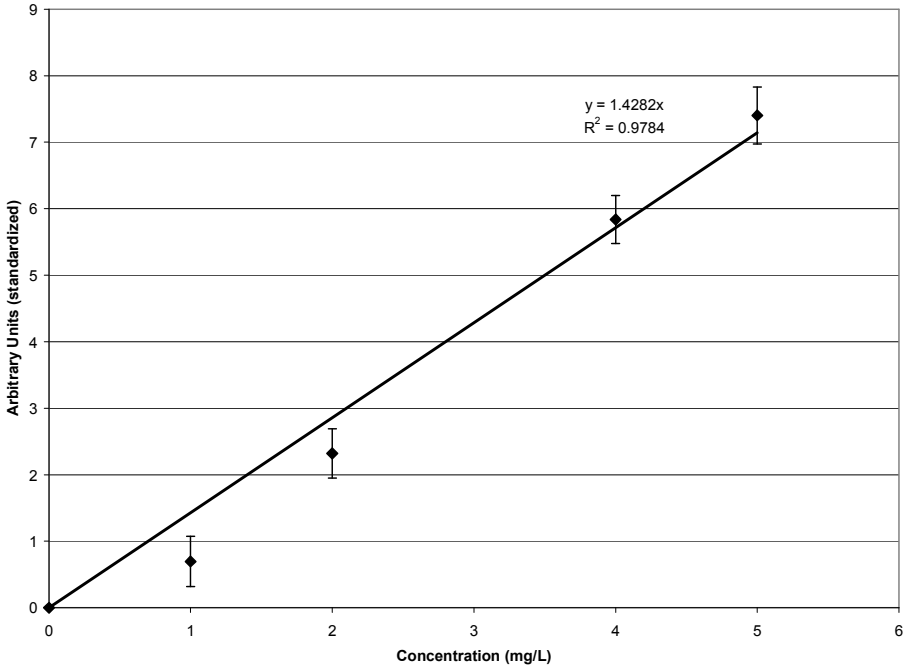

Figure A2.1: Calibration curve for the fluorescence detector

REFERENCES

Accardi-Dey, A., Gschwend, P.M. 2002. Assessing the Combine Roles of Natural Organic Matter and Black Carbon as Sorbents in Sediments. Environ. Sci. Technol. 36, 21-29.

Ahn, I., Ghiorse, W.C., Lion, L.W., Shuler, M.L. 1998. Growth Kinetics of *Pseudomonas putida* G7 on Naphthalene and Occurrence of Naphthalene Toxicity During Nutrient Deprivation. Biotechnol. Bioeng. 59, 587-594.

Aichberger, H., Loibner, A.P., Celis, R., Braun, R., Ottner, F., Rost, H. 2006. Assessment of Factors Governing Biodegradability of PAHs in Three Soils Aged Under Field Conditions. Soil and Sediment Contamination. 15, 73-85.

Aitken, M. Personal communication. 2006.

Amellal, N., Portal, J., Vogel, T., Berthelin, J. 2001. Distribution and Location of Polycyclic Aromatic Hydrocarbons (PAHs) and PAH-degrading Bacteria Within Polluted Soil Aggregates. Biodegradation. 12, 29-57.

Alexander, D.E., Fairbridge, R.W. 1999. Encyclopedia of Environmental Science. Kluwer Academic Publishers: Hingham.

Bird, R.B., Stewart, W.E., Lightfoot E.N. 1960. Transport Phenomena. John Wiley & Sons: New York.

Bosma, T.N., Middeldorp, P.J.M., Schraa, G., Zehnder, A.J.B. 1997. Mass Transfer Limitation of Biotransformation: Quantifying Bioavailability. Environ. Sci. Technol. 31, 248-252.

Carmichael, L.M., Christman, R.F., Pfaender, F.K. 1997. Desorption and Mineralization Kinetics of Phenanthrene and Chrysene in Contaminated Soils. Environ. Sci. Technol. 31, 126-132.

Carmichael, L.M., Pfaender, F.K. 1997. The Effect of Inorganic and Organic Supplememnts on the Microbial Degradation of Phenanthrene and Pyrene in Soils. Biodegradation. 8, 1-13.

Eriksson, M., Dalhammar, G., Mohn, W.W. 2002. Bacterial Growth and Biofilm Production on Pyrene. FEMS Microbiol. Ecol. 40, 21-27.

Fogler, H.S. 2006. Elements of Chemical Reaction Engineering. Prentice Hall: Upper Saddle River, NJ.

Ghosh, U., Gillette, J.S., Luthy, R., Zare, R.N. 2000. Microscale Location,

Characterization, and Association of Polycyclic Aromatic Hydrocarbons on Harbor Sediment Particles. Environ. Sci. Technol. 34, 1729-1736.

Gillette, J.S., Luthy, R.G., Clement, S.J., Zare, R.N. 1999. Direct Observation of Polycyclic Aromatic Hydrocarbons on Geosorbents at the Subparticle Scale. Environ. Sci. Technol. 33, 1185-1192.

Hunt, S.M., Werner, E.M., Huang, B., Hamilton, M.A., Stewart, P.S. 2004. Hypothesis for the Role of Nutrient Starvation in Biofilm Detachment. Appl. Environ. Microbiol. 70, 7418-7425.

Johnsen, A.R., Wick, L.Y., Harms, H. 2005. Principals of Microbial PAH-degradation in Soil. Environ. Pollut. 133, 71-84.

Luthy, R.G., Aiken, G.R., Brusseau, M.L., Cummingham, S.D., Gschwend, P.M., Pignatello, J.J., Reinhard, M., Traina, S.J., Weber, W.J., Westall, J.C. 1997. Sequestration of Hydrophobic Organic Contaminants by Geosorbents. Environ. Sci. Technol. 31, 3341-3347.

Manilal, V.B., Alexander, M. 1991. Factors Affecting the Microbial Degradation of Phenanthrene in Soil. Appl. Microbiol. Biotechnol. 35, 401-405.

Marx, R.B., Aitken, M.D. 1999. Quantification of Chemotaxis to Naphthalene by *Pseudomonas putida* G7. Appl. Environ. Microbiol. 65, 2847-2852.

Menzie, C.A., Potocki, B.B., Santodonato, J. 1992. Exposure to Carcinogenic PAHs in the Environment. Environ. Sci. Technol. 26, 1278-1284.

Milhelic, J.R., Lueking, D.R., Mitzell, R.J., Stapleton, J.M. 1993. Bioavailability of Sorbed- and Separate-phase Chemicals. Biodegradation. 4, 141-153.

Miller, J.H. 1972. Experiments in Molecular Genetics. Cold Spring Harbor, NY:Cold Spring Harbor Laboratory Press.

Mulder, H., Breure, A.M., Rulkens, W.H. 2001. Prediction of Complete Bioremediation Periods for PAH Soil Pollutants in Different Physical States by Mechanistic Models. Chemosphere. 43, 1085-1094.

Mulder, H., Breure, A.M., Van Andel, J.G., Grotenhuis, J.T.C., Rulkens, W.H. 1998a. Influence of Hydrodynamic Conditions on Naphthalene Dissolution and Subsequent Biodegradation. Biotechnol. Bioeng. 57, 145-154.

Mulder, H., Breure, A.M., Van Honschooten, D., Grotenhuis, J.T.C., Van Andel, J.G., Rulkens, W.H. 1998b. Effectof Biofilm Formation by Pseudomonas 8909N on the Bioavailability of Solid Naphthalene. Appl. Microbiol. Biotechnol. 50, 277-283.

Mulder, H., Wassink, G.R., Breure, A.M., Van Andel, J.G., Rulkens, W.H. 1998c. Effect of Nonionic Surfactants on Naphthalene Dissolution and Biodegradation. Biotechnol. Bioeng. 60, 397-407.

Nam, K. Alexander, M. 1998. Role of Nanoporosity and Hydrophobicity in Sequestration and Bioavailability: Tests with Model Solids. Environ. Sci. Technol. 32 71-74.

Purevdorj, B., Costerton, J.W., Stoodley, P. 2002. Influence of Hydrodynamics and Cell Signaling on the Structure and Behavoir of Pseudomonas aeruginosa Biofilms. Appl. Environ. Microbiol. 68, 4457-4464.

Rodrigues, A.C., Wuertz, S., Brito, A.G., Melo, L.F. 2003. Three-dimensional Distribution of GFP-labeled *Pseudomonas putida* during Biofilm Formation on Soild PAHs Assessed by Confocal Laser Scanning Microscopy. Water Sci. Technol. 47 139-142.

Stohs S.J., Ohia S., Bagchi D. 2002. Naphthalene toxicity and antioxidant nutrients. Toxicology 180, 97–105.

Stucki, G., Alexander, M. 1987. Role of Dissolution Rate and Solubility in Biodegradation of Aromatic Compounds. Appl. Envrion. Microbiol. 53, 292-297.

Tang, J., Carroquino, M.J., Robertson, B.K., Alexander, M. 1998. Combined Effect of Sequestration and Bioremediation in Reducing the Bioavailability of Polycyclic Aromatic Hydrocarbons in Soil. Environ. Sci. Technol. 32, 3586-3590.

Wick, L.Y., Colangelo, T., Harms, H. 2001. Kinetics of Mass Transfer-limited Bacterial Growth on Solid PAHs. Environ. Sci. Technol. 35, 354-361.

Wick, L.Y., de Munain, A.R., Springael, D., Harms, H. 2002. Responses of *Mycobacterium* sp. LB501T to the Low Bioavailability of Soild Anthracene. Appl. Microbiol. Biotechnol. 58, 378-385.

Wodzinski, R.S., Coyle, J.E. 1974. Physical State of Phenanthrene for Utilization by Bacteria. Appl. Microbiol. 27, 1081-1084.